Summation of free-energy diagrams of an anharmonic crystal and equation of state for a Lennard-Jones solid

Ramesh C. Shukla
Department of Physics, Brock University, St. Catharines, Ontario, Canada L2S 3A1

E. R. Cowley
Department of Physics, Camden College of Arts and Science, Rutgers University, Camden, New Jersey 08102-1205

(Received 13 August 1997)

We present a method of calculating the Helmholtz free energy of an anharmonic crystal. The exact expression for F, obtained by summing an infinite series of contributions, from *all* the loops and bubbles (quartic and cubic contributions to the self-energy of the Green's function), is evaluated numerically and the equation of state results for a Lennard-Jones solid are compared with the λ^2 perturbation theory (PT) which contains only the lowest order cubic and quartic contributions. It is shown that the infinite sum results are considerably improved over the λ^2 PT results for higher temperatures. Next we have presented a powerful ansatz approach of evaluating the same sum. The numerical results from this method are shown to be identical to the exact sum except at near T_m where they are very slightly different. The ansatz method is then extended to the higher order λ^4 diagrams and here too the numerical results are found to be improved over the results from the λ^4 PT. The ansatz procedure is then extended to the propagator renormalization and the numerical results obtained seem to have the best agreement with the results of classical Monte Carlo simulations. [S0163-1829(98)04729-8]

I. INTRODUCTION

The purpose of this paper is to report the equation of state results, for a fcc nearest-neighbor interaction Lennard-Jones (LJ) solid, from a procedure which requires the summation of an infinite series of diagrams, selected in a consistent manner. Our results are obtained in the classical or high-temperature (T) limit, $T>\Theta_D$ (the Debye temperature). The validity of the results obtained from the summation procedure is assessed by comparing them with the classical Monte Carlo (MC) results calculated for the same model potential.

We have been prompted to do this work because, as shown in Ref. 1, the straightforward application of the λ^2 perturbation theory (PT) (two diagrams) and even higher order λ^4 PT (eight additional diagrams) has produced divergence of almost all thermodynamic properties. This can be illustrated by the results for the heat capacity at constant volume (C_v). The classical MC calculation gives a value for C_v, that drops slightly as T increases from $3R$ at $T=0$ to about 88% of this at the melting temperature (T_m). The λ^2 PT result agrees at low T, up to 30% of T_m, and then drops sharply. The λ^4 PT result agrees with MC up to about 40% of T_m and then curves sharply *upwards*. From the point of view of divergence, the situation here seems to be similar to that encountered by Gell-Mann and Brueckner[2] in the calculation of the correlation energy of the electron gas.

One can get good agreement over a wider range of temperatures, either by leaving out some of the diagrams of $O(\lambda^4)$, as we did in Ref. 1, but for which *a priori* there is no basis other than achieving a good agreement, or, by summing diagrams to higher orders, ideally to an infinite order. However, if the summation is to be carried out, it should be done in a consistent manner, i.e., either *all* the diagrams in the same order of PT should be summed, or all the diagrams of similar magnitude but arising in different orders of PT should be summed. The former procedure has been followed by Choquard,[3] resulting in the first order self-consistent phonon theory (SC1) as well as others, e.g., SC2. But SC1 (Ref. 4) yields poor results and SC2 (Refs. 5,15) diverges. The latter procedure, where the diagrams are generated by the Van Hove ordering (λ) scheme,[6] has not been implemented, formally, or computationally and this is what we achieve in this paper in the classical limit.

As a first step, the diagrams of $O(\lambda^2)$ arising in the self-energy of the Green's function are summed in the determination of the Helmholtz free energy (F). This sum represents all the contributions to F from the loops and bubbles as inserts in the ring, to all orders of λ^2. The loops and bubbles are the only self-energy insertions of $O(\lambda^2)$. We are able to carry out this summation exactly. A comparison of the equation of state results from this calculation with that of the λ^2 PT (the most investigated anharmonic theory) will tell us about the importance of the higher order diagrams included in the summation procedure. To facilitate the presentation of our arguments, the free-energy and self-energy diagrams of $O(\lambda^2)$ and $O(\lambda^4)$ are presented in Figs. 1 and 2, respectively. The self-energy diagrams can be obtained by breaking one line in a free-energy diagram, but, in turn, the free-

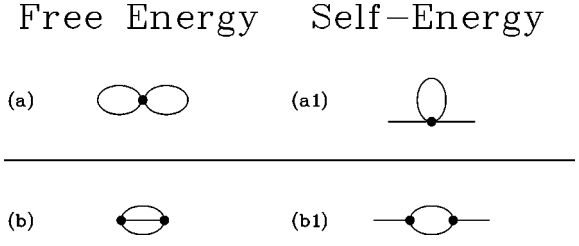

FIG. 1. Free energy and self-energy diagrams of order λ^2.

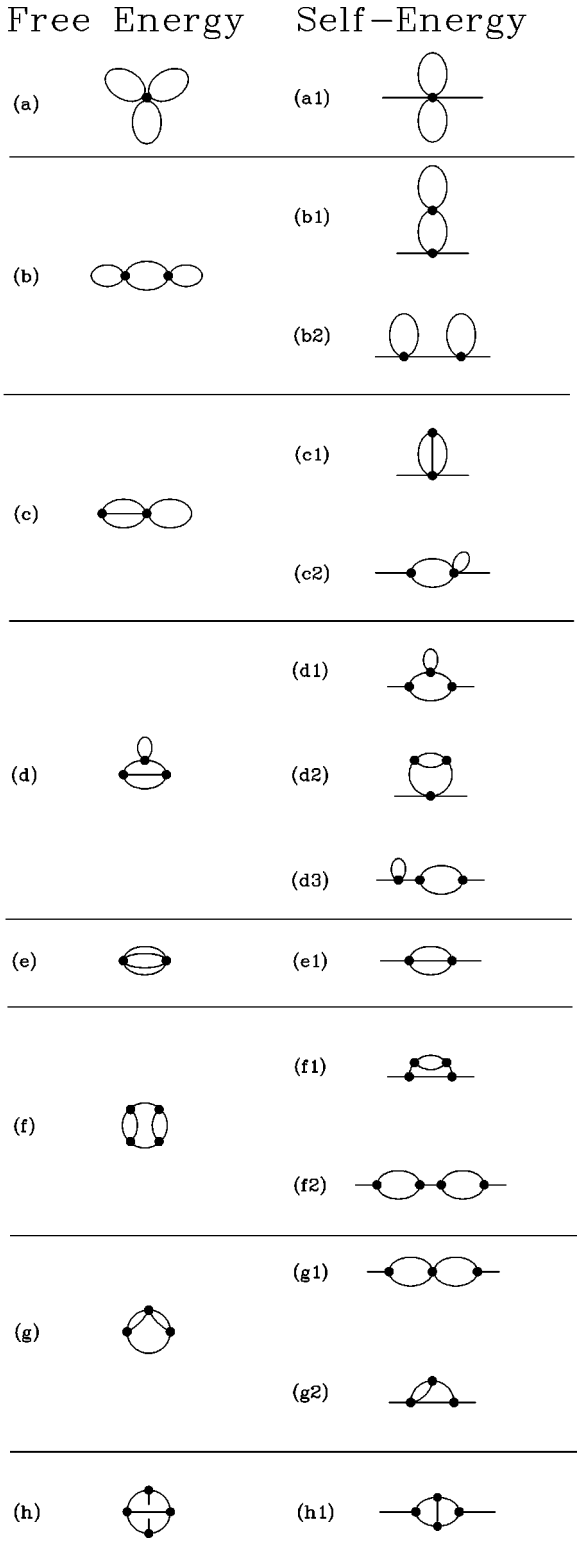

FIG. 2. Free energy and self-energy diagrams of order λ^4.

energy diagrams can often be interpreted as built from the self-energy diagrams as building blocks.

The next step in the summation procedure involves the insertions of the self-energy diagrams of $O(\lambda^4)$ in the ring. To avoid double counting in the total F up to $O(\lambda^4)$, the three diagrams (b), (d), and (f) in Fig. 2 are excluded from the summation procedure because these diagrams are already included in the first step through the self-energy insertions of $O(\lambda^2)$. We note that these three $O(\lambda^4)$ diagrams can be generated from the two $O(\lambda^2)$ diagrams, (a) and (b) of Fig. 1, by inserting either a loop or a bubble in the phonon lines in 1(a) and 1(b).

The last step in our calculation is the propagator renormalization. By this powerful procedure, even higher order diagrams than considered so far are generated by including self-energy inserts into internal phonon lines. When those lines themselves have inserts put into them, an iterative, or self-consistent, calculation is required. However, the number of terms generated in this way is enormous and their exact numerical evaluation for every wave vector ($\mathbf{q}$) and branch index (j), in some reasonable time, is very difficult, if not impossible. Thus, due to the extreme complexity of these calculations, largely due to the tensorial character of the anharmonic force constants, their Fourier transforms, multiple Brillouin zone (BZ) summations restricted by numerous Δ functions, and finally neighbor summations, we have developed an ansatz to approximate many such diagrams as products of simpler diagrams, with numerical factors. In the situations where we can compare these results with exact calculations, they have been found to be amazingly accurate. We therefore apply this technique to give equation of state results when the internal propagator lines are treated to different degrees of sophistication. Some of the approximations developed in this way lie very close to the MC results over the entire temperature range of the solid.

II. INFINITE SUMMATION OF ALL THE RING DIAGRAMS INVOLVING THE LOOP AND BUBBLE INSERTS

The infinite series of all the ring diagrams, involving the loop and bubble inserts, can be summed in closed form by the following procedure which involves modifying the multiplying coefficient of the $A^{\dagger}_{\mathbf{q}j}A_{\mathbf{q}j}$ operators in the Hamiltonian (H) and then a subsequent integration over a coupling parameter (g), $0 \leqslant g \leqslant 1$. The procedure also requires the knowledge of the one phonon Green's function which can be derived by the diagrammatic method[7,8] or by the Zubarev prescription.[9,10] Here we have followed the Zubarev method because it has a built-in self-consistency criterion. Then for the H containing the harmonic and anharmonic (cubic and quartic) contributions, the one phonon Green's function in the diagonal approximation is given by

$$G^{jj'}_{\mathbf{qq}'} = \frac{2\omega_{\mathbf{q}j}\delta_{\mathbf{qq}'}\delta_{jj'}}{2\pi[\omega^2 - \Omega^2_{\mathbf{q}j}(\omega)]}, \tag{1}$$

where $\Omega^2_{\mathbf{q}j}(\omega)$ is in general a frequency-dependent renormalized phonon frequency and its complete expresson can be found in Ref. 10. However, in the context of the evaluations of the anharmonic contributions to the average square of the atomic displacement[11] and F (Ref. 12) it has been shown that the ω dependence of $\Omega^2_{\mathbf{q}j}(\omega)$ in the high-temperature limit is not very important because exact results for these quantities are given in this limit when $\Omega^2_{\mathbf{q}j}(\omega)$ is evaluated at $\omega = 0$ which we simply denote as $\Omega^2_{\mathbf{q}j}$. Thus, from Eqs. (15)–(17) of Ref. 12, we have

$$\Omega^2_{\mathbf{q}j} = \omega^2_{\mathbf{q}j} + D_3(\mathbf{q}j) + D_4(\mathbf{q}j), \tag{2}$$

$$D_3(\mathbf{q}j) = -\frac{\lambda^2}{2\beta N}\sum_{\mathbf{q}_1 j_1}\sum_{\mathbf{q}_2 j_2}\Delta(-\mathbf{q}+\mathbf{q}_1+\mathbf{q}_2) \times \frac{|\Phi(-\mathbf{q}j,\mathbf{q}_1 j_1,\mathbf{q}_2 j_2)|^2}{\Omega^2_{\mathbf{q}_1 j_1}\Omega^2_{\mathbf{q}_2 j_2}}, \tag{3}$$

$$D_4(\mathbf{q}j) = \frac{\lambda^2}{2\beta N}\sum_{\mathbf{q}_1 j_1}\frac{\Phi(\mathbf{q}_1 j_1,-\mathbf{q}_1 j_1,\mathbf{q}j,-\mathbf{q}j)}{\Omega^2_{\mathbf{q}_1 j_1}}, \tag{4}$$

where we have replaced $\omega_{\mathbf{q}j}$ in the right-hand side of Eqs. (16) and (17) of Ref. 12, with $\Omega_{\mathbf{q}j}$. We note that $\Omega^2_{\mathbf{q}j}$ can be determined only self-consistently from Eqs. (2)–(4) because of the appearance of $\Omega^2_{\mathbf{q}j}$ in the denominators of the right-hand sides of Eqs. (3) and (4). The above equations can be derived rigourously in the high-temperature limit with the self-consistency condition built in the Zubarev method. In Eqs. (1)–(4) the various symbols have the following meaning: $\beta = 1/k_B T$, where k_B is the Boltzmann constant, $\Phi(-\mathbf{q}j,\mathbf{q}_1 j_1,\mathbf{q}_2 j_2)$ and $\Phi(\mathbf{q}_1 j_1,-\mathbf{q}_1 j_1,\mathbf{q}_2 j_2,-\mathbf{q}_2 j_2)$ are the Fourier transforms of the third and fourth rank tensors, respectively, and N represents the number of unit cells in the crystal.

We have solved these equations exactly. However, it is useful to develop an approximate solution to make contact with some ideas to be discusssed in the next section. An approximate self-consistent solution can be obtained by substituting

$$\Omega^2_{\mathbf{q}j} = \omega^2_{\mathbf{q}j}(1+X) \tag{5}$$

in Eqs. (2)–(4), where the average quantity $X = (1/3N)\Sigma_{\mathbf{q}j} X_{\mathbf{q}j}$ with $X_{\mathbf{q}j} = [D_3(\mathbf{q}j) + D_4(\mathbf{q}j)]/\omega^2_{\mathbf{q}j}$, is calculated from

$$X = \frac{2}{3Nk_B T}\left[2\frac{F_{1a}}{1+X} + 3\frac{F_{1b}}{(1+X)^2}\right], \tag{6}$$

where F_{1a} and F_{1b} are the free energies for the diagrams of $O(\lambda^2)$ in Fig. 1. In terms of the matrices $A(\mathbf{q}jj')$ and $B(\mathbf{q}jj')$

$$A(\mathbf{q}jj') = \frac{1}{N\omega_{\mathbf{q}j}\omega_{\mathbf{q}j'}}\sum_{\mathbf{q}_1 j_1}\frac{\Phi(\mathbf{q}_1 j_1,-\mathbf{q}_1 j_1,\mathbf{q}j,-\mathbf{q}j')}{\omega^2_{\mathbf{q}_1 j_1}}, \tag{7}$$

$$B(\mathbf{q}jj') = \frac{1}{N\omega_{\mathbf{q}j}\omega_{\mathbf{q}j'}}\sum_{\mathbf{q}_1 j_1}\sum_{\mathbf{q}_2 j_2}\Delta(-\mathbf{q}+\mathbf{q}_1+\mathbf{q}_2) \times \frac{\Phi(-\mathbf{q}j,\mathbf{q}_1 j_1,\mathbf{q}_2 j_2)\Phi(-\mathbf{q}_1 j_1,-\mathbf{q}_2 j_2,\mathbf{q}j')}{\omega^2_{\mathbf{q}_1 j_1}\omega^2_{\mathbf{q}_2 j_2}}, \tag{8}$$

F_{1a} and F_{1b} are given by

$$F_{1a} = \frac{1}{8N\beta^2}\sum_{\mathbf{q}j} A(\mathbf{q}jj), \tag{9}$$

$$F_{1b} = -\frac{1}{12N\beta^2}\sum_{\mathbf{q}j} B(\mathbf{q}jj). \tag{10}$$

Since the Green's function, expressed in terms of $\Omega^2_{\mathbf{q}j}$, as given by Eq. (1) is identical in mathematical structure to the Green's function for a harmonic system we can write an equivalent harmonic form for the anharmonic H. This form in terms of the modified coefficient for the operator $A^\dagger_{\mathbf{q}j}A_{\mathbf{q}j}$, is given by

$$H = \frac{\hbar}{4}\sum_{\mathbf{q}j}\left[\frac{\Omega^2_{\mathbf{q}j}}{\omega_{\mathbf{q}j}}A^\dagger_{\mathbf{q}j}A_{\mathbf{q}j} + \omega_{\mathbf{q}j}B^\dagger_{\mathbf{q}j}B_{\mathbf{q}j}\right] \tag{11}$$

$$= \sum_{\mathbf{q}j}\frac{\hbar\omega_{\mathbf{q}j}}{4}(A^\dagger_{\mathbf{q}j}A_{\mathbf{q}j} + B^\dagger_{\mathbf{q}j}B_{\mathbf{q}j}) + g\frac{\hbar}{4}\sum_{\mathbf{q}j}\frac{(\Omega^2_{\mathbf{q}j}-\omega^2_{\mathbf{q}j})}{\omega_{\mathbf{q}j}}A^\dagger_{\mathbf{q}j}A_{\mathbf{q}j}, \tag{12}$$

where we have multiplied the second term of Eq. (12) with a coupling constant g for the purpose of evaluating F by the method of integration over the coupling constant. The advantage of writing H in the form of Eq. (12) is that we can consider the second term as an interaction term between the phonon modes $\mathbf{q}$ and j and the Hamiltonian is of the same mathematical structure as that of the interacting Einstein oscillators[13] where the free energy was evalulated by the coupling constant integration method and in another paper[14] it was shown to be equivalent to the results obtained from the ring diagram summation procedure. However, when these same methods are applied in the present problem we have some ambiguity in the definitions of vertex and ring. Unlike the case of interacting Einstein oscillators where the vertex was a simple vertex with no structure, here the vertex is complicated and has a stucture. This structure is defined as the sum of quartic and cubic vertices each of them consisting of a loop and a bubble, respectively. Therefore when the lines are folded to form a ring the ambiguity arises in the lowest order in the definition of the ring and the insert. Thus we expect the first order insert contributions to be corrected for the numerical factors when the above method is applied in the present problem. Thus employing the coupling constant integration method,[13] F is given by

$$F = \frac{1}{\beta}\sum_{\mathbf{q}j}\ln\left(2\sinh\frac{1}{2}\beta\hbar\Omega_{\mathbf{q}j}\right). \tag{13}$$

Since our calculations are done in the classical limit, we can isolate the terms which are independent of $\hbar$ with the help of the standard product representation for $\sinh x/x$, with $x = \frac{1}{2}\beta\hbar\Omega_{\mathbf{q}j}$. The result is that the terms which depend on $\hbar$ and the $\hbar$ independent terms are separated in the following manner:

$$F = \frac{1}{\beta}\sum_{\mathbf{q}j}\ln(\beta\hbar\omega_{\mathbf{q}j}) + \frac{1}{2\beta}\sum_{\mathbf{q}j}\ln\left[1+\frac{D_3(\mathbf{q}j)+D_4(\mathbf{q}j)}{\omega^2_{\mathbf{q}j}}\right] + \frac{1}{\beta}\sum_{\mathbf{q}j}\sum_{n=1}^{\infty}\ln\left[1+\frac{\beta^2\hbar^2\Omega^2_{\mathbf{q}j}}{4n^2\pi^2}\right]. \tag{14}$$

The substitution of $D_3(\mathbf{q}j)$, $D_4(\mathbf{q}j)$, and $\Omega^2_{\mathbf{q}j}$ from Eqs. (3), (4), and (5), respectively, into Eq. (14) yields the following $\hbar$ independent anharmonic contribution to F which does not include the effect of renormalization of the phonon frequencies ($X=0$):

$$F_A=\frac{1}{2\beta}\sum_{\mathbf{q}j}\ \ln\left[1+\frac{\lambda^2}{2\beta}A(\mathbf{q}jj)-\frac{\lambda^2}{2\beta}B(\mathbf{q}jj)\right], \quad (15)$$

where A and B are given by Eqs. (7) and (8). By expanding the ln function in Eq. (15), we can identify the standard cubic (F_3) and quartic (F_4) contributions, after summing over $\mathbf{q}$ and j, as those arising from the first term of the expansion. Compared to the correct expression (obtained by other methods) the present F_3 and F_4 differ by factors of $\frac{1}{3}$ and $\frac{1}{2}$, respectively. The other higher order contributions of $O(\lambda^4)$, such as (b), (d), and (f) in Fig. 2 and other diagrams of these types of $O(\lambda^6)$, $O(\lambda^8)$, etc., are correctly given. We also note that in deriving Eq. (15) the mixing of phonon modes j and j' has not been allowed and for simplicity only the diagonal contributions of $A(\mathbf{q}jj')$ and $B(\mathbf{q}jj')$ matrices have been included in the calculations. When this mixing in j and j' is allowed the anharmonic contribution [the second term of Eq. (14)] gets modified. Taking this effect into account and the differences in the numerical factors of F_3 and F_4 the final correct expression for the total anharmonic contribution (F_A) to F, which we have employed in our calculations, is given by

$$F_A=-F_{1(a)}-2F_{1(b)}+\frac{1}{2\beta}\sum_{\mathbf{q}}\ \mathrm{Tr}\ \ln\left(I+\frac{1}{2\beta}M\right), \quad (16)$$

where in Eq. (16) Tr stands for the trace operation, I is a 3×3 unit matrix, and the matrix M is given by $M(\mathbf{q}jj')=A(\mathbf{q}jj')-B(\mathbf{q}jj')$, where A and B are defined by Eqs. (7) and (8).

When the effect of renormalization is included, Eq. (15) is replaced by the following expression for the anharmonic free energy:

$$F_A=\frac{1}{2\beta}\sum_{\mathbf{q}j}\ \ln\left[1+\frac{\lambda^2}{2\beta}\frac{A(\mathbf{q}jj)}{1+X}-\frac{\lambda^2}{2\beta}\frac{B(\mathbf{q}jj)}{(1+X)^2}\right]$$
$$-\frac{F_{1(a)}}{1+X}-\frac{2F_{1(b)}}{(1+X)^2}. \quad (17)$$

However, if we use the fully renormalized frequencies as determined by the iterative solution of Eq. (6), the last two terms in Eq. (17) will be modified to $-F_{1(a)}/(1+X)^2-2F_{1(b)}/(1+X)^3$ because as seen from the expressions for $F_{1(a)}$ and $F_{1(b)}$ each $\omega_{\mathbf{q}j}$ in the denominator is then replaced by $\omega^2_{\mathbf{q}j}(1+X)$. A further discussion of this point in the numerical calculations to $O(\lambda^2)$ as well as $O(\lambda^4)$ is given in the next section.

III. AN APPROXIMATE SUM OF HIGHER ORDER DIAGRAMS

In the approximate method of summing the higher order diagrams, or ansatz, we replace $A(\mathbf{q}jj)$ and $B(\mathbf{q}jj)$ in Eq. (17), by their average values in terms of $F_{1(a)}$ and $F_{1(b)}$, from Eqs. (9) and (10) and set $X=0$. The averages are calculated from the same definition as given earlier in the calculation of X. Thus Eq. (17) reduces to

$$F_A=\frac{3Nk_BT}{2}\ln\left\{1+\frac{4F_{1(a)}}{3Nk_BT}+\frac{2F_{1(b)}}{Nk_BT}\right\}-F_{1(a)}-2F_{1(b)}. \quad (18)$$

We note here the following important result: whereas the diagrams 2(b), 2(d), and 2(f) of $O(\lambda^4)$ were exactly included in Eq. (15) now we find from the second term of the expansion of the ln function of Eq. (18)

$$F_{2(b)}\simeq-\frac{4}{3}\frac{F^2_{1(a)}}{Nk_BT}, \quad (19)$$

$$F_{2(d)}\simeq-4\frac{F_{1(a)}F_{1(b)}}{Nk_BT}, \quad (20)$$

$$F_{2(f)}\simeq-3\frac{(F_{1(b)})^2}{Nk_BT}. \quad (21)$$

Compared to the exact numerical values of $F_{2(b)}$, $F_{2(d)}$, and $F_{2(f)}$ the errors from the above expressions for these diagrams are about 1–3 % for $F_{2(b)}$, 0.4–1.5 % for $F_{2(d)}$, and 1.25–2.2 % for $F_{2(f)}$. In each case, the actual discrepancy depends slightly on the volume. This combination of diagrams corresponds to what we have called the exact sum. We can therefore test the ansatz at this stage by evaluating the equation of state using both Eq. (18) and the exact sum, Eq. (16). The agreement is very good. We believe it will be worthwhile to use the approximations given here in calculations on more elaborate models. Only the two lowest order diagrams need to be evaluated exactly and the sum of an infinite number of ring diagrams can then be approximated.

So far, we have been able to test each approximation that we have developed from the numerical results to order λ^2 and λ^4. We now wish to use the remaining results of order λ^4 to estimate other higher order terms. First, we rewrite the sum of ring diagrams as

$$F_A=\frac{3Nk_BT}{2}\ln\{1+x\}-F_{1(a)}-2F_{1(b)},$$

where

$$x=\frac{4F_{1(a)}}{3Nk_BT}+\frac{2F_{1(b)}}{Nk_BT}.$$

From a comparison with the expression for the exact logarithmic sum, we see that the quantity x plays the role of an average squared frequency shift. That is, if the harmonic squared frequencies were all multiplied by the same factor $(1+x)$, the logarithmic contribution to the free energy would have the form that we suggest. There is a simple relationship between the contributions to the free energy and the related contributions to the average shift x, that each shift contribution equals the free-energy contribution, divided by $3Nk_BT/2$, and multiplied by the number of lines that can be cut to convert the free-energy diagram to a self-energy diagram.

Using this rule, we can construct the contributions to the free energy arising from ring diagrams with inserts developed from diagrams 2(c), 2(e), 2(g), and 2(h). The numbers of lines that can be cut in these cases are 4, 4, 5, and 6, respectively. Diagrams 2(b), 2(d), and 2(f) have already been included partially. However, they make additional contributions. The self-energy diagrams obtained by cutting each of the lines in a free-energy diagram are shown in Figs. 1 and 2. In the cases 2(b), 2(d), and 2(f), one of the diagrams generated in this way is improper. That is, it can be split into two diagrams by the cutting of a single line. It is these improper diagrams whose contributions to the self-energy have been estimated. There are additional contributions that are estimated using the above rule, except that the numerical factor is the number of lines that can be cut to give a proper diagram. In this way, we arrive at an expression for the anharmonic contribution to the free energy of

$$F_A=\frac{3Nk_BT}{2}\ln\{1+x\}-F_{1(a)}-2F_{1(b)}-2F_{2(a)}-2F_{2(b)}-3F_{2(c)}-3F_{2(d)}-3F_{2(e)}-4F_{2(f)}-4F_{2(g)}-5F_{2(h)}, \tag{22}$$

$$x=\frac{2}{3Nk_BT}\{2F_{1(a)}+3F_{1(b)}+3F_{2(a)}+2F_{2(b)}+4F_{2(c)}+3F_{2(d)}+4F_{2(e)}+4F_{2(f)}+5F_{2(g)}+6F_{2(h)}\}. \tag{23}$$

This expression sums the anharmonic contribution to the free energy arising from all ring diagrams with inserts up to order λ^4. To this accuracy, the only approximations are Eqs. (19)–(21) which we know are well satisfied numerically.

The identification of the quantity x with an average shift in the squared frequency suggests another extension of the classes of diagrams that can be summed. As described earlier, many diagrams, such as the subset 2(b), 2(d), and 2(f), can be interpreted as simpler diagrams with self-energy inserts in some of the lines. The explicit expression, Eq. (4), for the contribution to the self-energy arising from diagram (a1) of Fig. 1 contains a squared phonon frequency in the denominator, and the contribution from diagram (b1) of Fig. 1, Eq. (3), contains two squared frequencies in the denominator. If we divide these contributions by factors of $(1+x)$ and $(1+x)^2$, respectively, then we are mimicking the effect of the self-energy of the intermediate phonons. For consistency, in Eq. (22) each term must be divided by as many factors of $(1+x)$ as there are lines in the corresponding diagram. We find that, to order λ^4, the contributions to x and to the free energy from diagrams 2(b), 2(d), and 2(f) are fully included if we write

$$F_A=\frac{3Nk_BT}{2}\ln\{1+x\}-\frac{F_{1(a)}}{(1+x)^2}-2\frac{F_{1(b)}}{(1+x)^3}-2\frac{F_{2(a)}}{(1+x)^3}-3\frac{F_{2(c)}}{(1+x)^4}-3\frac{F_{2(e)}}{(1+x)^4}-4\frac{F_{2(g)}}{(1+x)^5}-5\frac{F_{2(h)}}{(1+x)^6}, \tag{24}$$

$$x=\frac{2}{3Nk_BT}\left\{2\frac{F_{1(a)}}{(1+x)}+3\frac{F_{1(b)}}{(1+x)^2}+3\frac{F_{2(a)}}{(1+x)^2}+4\frac{F_{2(c)}}{(1+x)^3}+4\frac{F_{2(e)}}{(1+x)^3}+5\frac{F_{2(g)}}{(1+x)^4}+6\frac{F_{2(h)}}{(1+x)^5}\right\}. \tag{25}$$

We have also used Eqs. (19)–(21) once more. Note that there is now no explicit contribution from diagrams 2(b), 2(d), and 2(f). A significant feature of this approximation is that the quantity x appears on both sides of the equation. It must therefore be determined consistently, for example by iteration. The self-consistent value of x models, in an average sense, the shift in the phonon frequencies in self-consistent phonon theories. The results of calculations using Eqs. (24) and (25) are labeled ansatz/$(1+x)$ in the figures. This set of equations sums the contributions from all ring diagrams with any number of self-energy inserts of order up to λ^4, to the extent that the numerical approximations are valid.

IV. RESULTS AND DISCUSSION

As indicated in the earlier sections of this paper we have carried out several calculations of the equation of state for a nearest-neighbor model of the fcc LJ solid and compared them with the classical MC results also obtained for the same model potential. As described in Ref. 1, the lattice sums were evaluated for a range of volumes and the thermal properties then found by suitable interpolations and differentiations.

We have calculated the nearest-neighbor distance (R/σ), zero pressure constant-volume specific heat (C_V), isothermal bulk modulus (B_T), thermal expansivity (β_P), and the specific heat at constant pressure (C_P) for several λ^2 and λ^4 theories with propagator renormalization effects included. Since most of these properties behave in a similar fashion as far as the agreement with MC is concerned, we have presented graphically only values of C_v as a representative curve for the various λ^2 theories and C_P, (R/σ), B_T from the λ^4 theories considered in this paper. Figure 3 represents the results of our calculations for the quasiharmonic (QH), the classical λ^2 PT, λ^2 ansatz, (λ^2 ansatz)/$(1+x)$, exact sum (ES). Figures 4–6 represent the results for the classical λ^4 PT, λ^4 ansatz, the logarithmic ansatz with propagator renormalization (λ^4 ansatz)/$(1+x)$, λ^4-ladder theory [which means taking into account all the diagrams up to $O(\lambda^4)$ except the Ladder diagram 2(h)], and finally the λ^4-ladder with propagator renormalization [(λ^4-ladder)/$(1+x)$]. In all cases the comparison is made with the MC values obtained for $N=256$ atoms[16] with the $N-1$ correction applied to the vibrational contributions. These results are in very good agreement with the earlier MC results for 108 atoms.[17]

It is clear from these results that the QH curves for all the properties shift significantly when the λ^2 PT contributions are included. The further addition of *all* the λ^4 contributions again produces a significant shift in the curves in the opposite direction. The divergence of the λ^2 PT from about $0.3T_m$ has now moved to $0.4T_m$. Among the various options considered involving the λ^2 theory, although considerable improvement is seen in the results of λ^2 ansatz over the λ^2 PT, the best set of results are given by the (λ^2 ansatz)/$(1+x)$ theory. Now when all the contributions to $O(\lambda^4)$ are

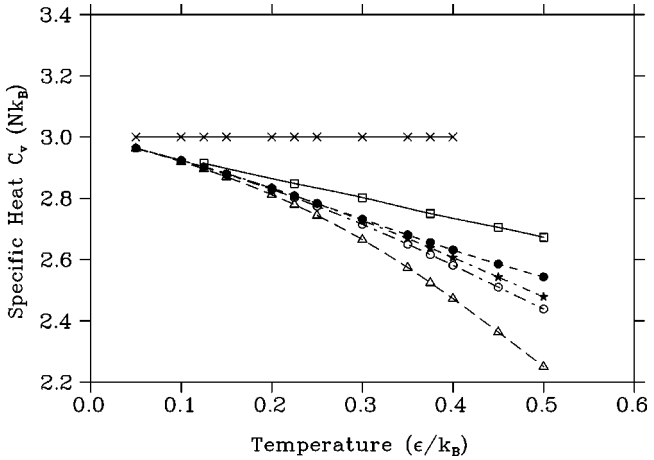

FIG. 3. Specific heat at constant volume (C_V) from λ^2 diagrams. Symbols are $\times$: quasiharmonic, $\triangle$: λ^2 perturbation theory, $\bigcirc$: λ^2 ansatz, $\bullet$: λ^2 ansatz/(1+x), $\star$: exact sum, $\square$: Monte Carlo.

summed to infinity we have the results given in λ^4 ansatz. The curves are much better behaved and yield a good agreement with the MC curves approximately up to $0.6T_m$ but then again the divergence sets in. The (λ^4 ansatz)/$(1+x)$ procedure pushes the good agreement up to $0.75T_m$ before the results start diverging. It is also interesting to note that the λ^4-ladder results, which are exact calculations, hold very well up to $0.9T_m$ before the onset of the divergence. When compared with the classical λ^4 results it seems that the cause of the divergence of the $O(\lambda^4)$ PT at an earlier stage in the calculation is due to the ladder diagram. Clearly almost complete agreement with MC is achieved with the (λ^4-ladder)/$(1+x)$ approach.

V. CONCLUSIONS

We have presented a method of deriving the Helmholtz free energy of an anharmonic crystal where an infinite set of diagrams, consisting of any number of loops and bubbles in individual form and in *all* possible combinations, are summed to infinity. We have also presented a powerful ansatz approach of summing the same set of diagrams. The numerical results in the classical limit for the equation of state of an fcc LJ solid (with nearest-neighbor interaction) are indistinguishable from each other. Thus after testing the validity of the ansatz method vis-à-vis the exact results the method is extended to include *all* the higher order contributions of $O(\lambda^4)$. The infinite set of contributions to F from *all* the self-energies of $O(\lambda^4)$ is then evaluated for the calculation of the equation of state. The method is then extended to include the propagator renormalization. Since we have compared all of our results with the MC method also calculated for the same model, in several instances our results agree almost exactly with those of MC. In short, we have exhausted *all* possibilities of selecting diagrams of at least up to $O(\lambda^4)$ as well as the infinite series of such diagrams.

Since our objective in this paper has been to select a group of diagrams of the same order of magnitude generated via the Van Hove ordering scheme and sum them to infinity, we have achieved this objective in a consistent manner. Compared to the traditional manybody work where the vertices are usually taken as constants our work here has been more difficult because of the tensorial character of the force constants, their Fourier transforms, multiple Brillouin zone, and neighbor summations. However when all is said and

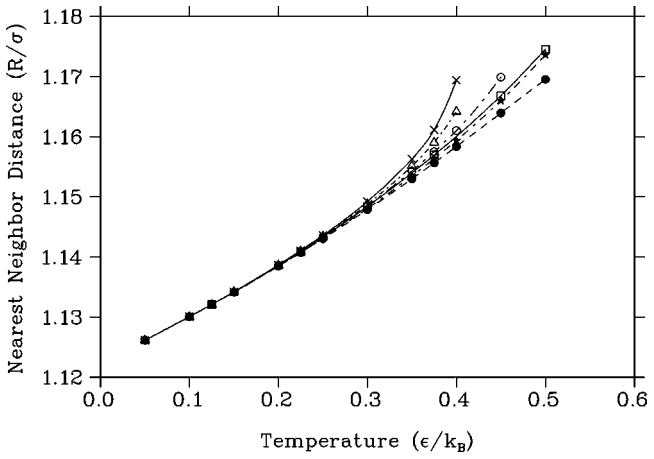

FIG. 4. Nearest-neighbor distance R including contributions from λ^4 diagrams. Symbols are $\times$: λ^4 perturbation theory, $\triangle$: λ^4 ansatz, $\bigcirc$: λ^4 ansatz/(1+x), $\bullet$: λ^4-ladder, $\star$: (λ^4 ansatz - ladder)/(1+x), $\square$: Monte Carlo.

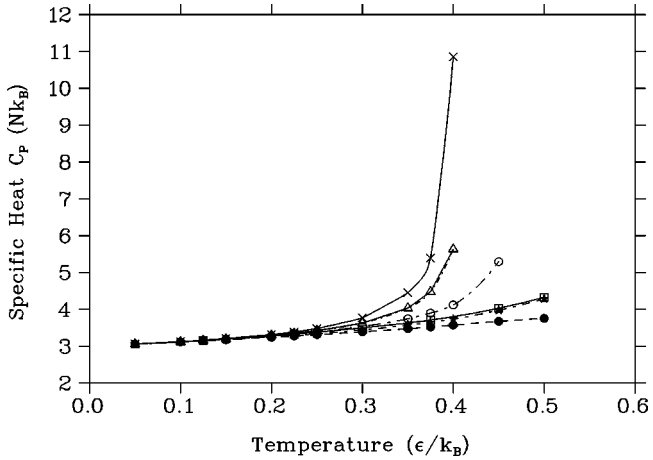

FIG. 5. Specific heat at constant pressure (C_P). Symbols as in Fig. 4.

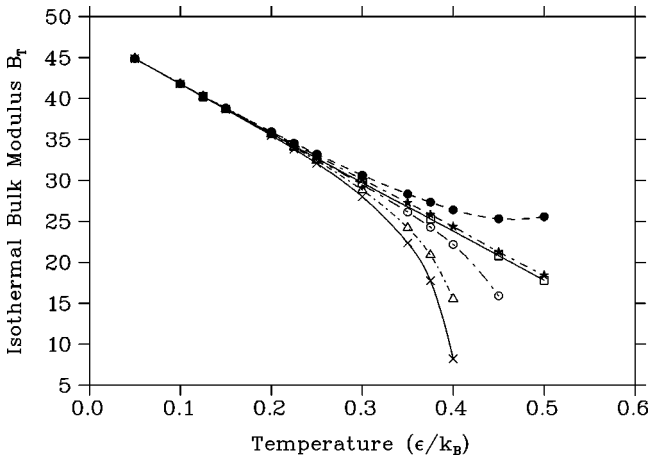

FIG. 6. Isothermal bulk modulus (B_T). Symbols as in Fig. 4.

done we have just about achieved our purpose in exhausting *all* possibilities of selecting and summing these diagrams for an anharmonic crystal. The agreement with MC in the classical high-temperature limit is very good in some cases and we believe that this is as best as it can be done at present from an analytical theory.

ACKNOWLEDGMENTS

One of us (R.C.S.) wishes to acknowledge the support of the Natural Sciences and Engineering Research Council of Canada. The authors acknowledge the help provided by Ronald Snelgrove in drawing the various figures of this paper.

[1] R. C. Shukla and E. R. Cowley, Phys. Rev. B **31**, 372 (1985).
[2] M. Gell-Mann and K. Brueckner, Phys. Rev. **106**, 364 (1957).
[3] P. F. Choquard, *The Anharmonic Crystal* (Benjamin, New York, 1967).
[4] N. S. Gillis, N. R. Werthamer, and T. R. Koehler, Phys. Rev. **165**, 951 (1968).
[5] L. B. Kanney and G. K. Horton, Fiz. Nizk. Temp. **1**, 739 (1975) [Sov. J. Low Temp. Phys. **1**, 356 (1975)].
[6] L. Van Hove, *Quantum Theory of Many Particle Systems* (Benjamin, New York, 1961).
[7] A. A. Maradudin and A. E. Fein, Phys. Rev. **128**, 2589 (1962).
[8] R. A. Cowley, Adv. Phys. **12**, 421 (1963).
[9] D. N. Zubarev, Usp. Fiz. Nauk **71**, 71 (1960) [Sov. Phys. Usp. **3**, 320 (1960).
[10] R. C. Shukla and E. R. Muller, Phys. Status Solidi B **43**, 413 (1971).
[11] R. C. Shukla and H. Hübschle, Phys. Rev. B **40**, 1555 (1989).
[12] R. C. Shukla and E. Sternin, Philos. Mag. B **74**, 1 (1996).
[13] R. C. Shukla and E. R. Muller, Am. J. Phys. **39**, 77 (1971).
[14] R. C. Shukla and E. R. Muller, Am. J. Phys. **40**, 504 (1972).
[15] E. R. Cowley, G. K. Horton, and J. G. Leese, in *Proceedings of the Second International Conference on Phonon Physics*, Budapest, Hungary, 1985, edited by J. Kollar *et al.* (World Scientific, Singapore, 1985).
[16] R. C. Shukla, F. Boseglav, and J. C. Whybra (unpublished).
[17] E. R. Cowley, Phys. Rev. B **28**, 3160 (1983); M. A. Day and R. J. Hardy, J. Phys. Chem. Solids **46**, 487 (1985).